Multi-user downlink NOMA systems aided by an ambient backscatter device: achievable rate region and energy-efficiency maximization

Hajar El Hassani, Anne Savard, E. Veronica Belmega, Rodrigo C. De Lamare

Multi-user downlink NOMA systems aided by ambient backscattering: achievable rate regions and energy-efficiency maximization

Hajar El Hassani, *Student Member, IEEE,* Anne Savard, *Member, IEEE,* E. Veronica Belmega, *Senior Member, IEEE,* and Rodrigo C. de Lamare, *Senior Member, IEEE*

***Abstract*—In this paper, we investigate the energy efficiency of a multi-user downlink non-orthogonal multiple access (NOMA) system aided by an ambient backscatter device that modulates its own information by reflecting the incident signal coming from the NOMA transmitter. Because of the multiplicative operation at the ambient backscatter device when reflecting the transmitter's signal, the achievable sum rate of the system is not known. Hence, we first derive the information-theoretic achievable rate region for a discrete memoryless channel and, subsequently, for Gaussian channels. We then propose a joint optimization framework for maximizing the system energy efficiency as the tradeoff and ratio between the overall sum rate and the power consumption, under user minimum rate constraints. For this, we propose a modification that simplifies the resulting non-convex optimization problems, which enables us to obtain the optimal reflection coefficient and power allocation policy analytically (up to a one line search). Numerical results demonstrate the negligible impact of the introduced modification on the optimality of our solution. Remarkably, our results show that the ambient backscatter-aided NOMA significantly outperforms OMA: the relative gain increases with the number of receivers, reaching up to $14\times$ improvement over OMA. At last, we show the pertinence of our solution also under imperfect channel state information.**

***Index Terms*—Non-orthogonal multiple access (NOMA), ambient backscatter communication (AmBC), internet of things (IoT), information-theoretic achievable rate region, energy-efficiency optimization**

I. Introduction

Recent advances in wireless communications have paved the way to the internet of things (IoT), connecting an immense number of devices. Since this number is projected to increase every year, so do the challenges and requirements to achieve massive connectivity, extended battery life and higher energy efficiency [2]. One of the promising technologies for alleviating the radio resources scarcity and enabling massive connectivity is non-orthogonal multiple access (NOMA) which, unlike conventional orthogonal multiple access techniques (OMA), allows the simultaneous communications via the same radio resources (e.g., frequency bands, time slots, etc.). In power-domain NOMA, the multiple access interference is overcome via two fundamental techniques: *superposition coding* at the transmitter, such that the messages are encoded in a layered manner and sent with different power levels, and *successive interference cancellation* (SIC) at the receivers, such that the strongest received signals are decoded first (by treating weaker signals as noise) in a successive manner until the intended signal is retrieved [3–5].

The energy efficiency, a key performance indicator for the sixth generation (6G) wireless communications, is a growing concern especially for IoT networks, in which a significant amount of energy is consumed to ensure the quality of service (QoS) requirements of different services and applications. 6G networks are expected to improve the energy efficiency by a factor of $10 - 100$ times with respect to (w.r.t.) the fifth generation (5G) wireless networks [2]. Moreover, the deployment of thousands of stations (base stations (BS), small-cells, relays, etc.) needed for IoT networks will result in huge power consumption and carbon emissions [6]. Consequently, developing energy-efficient systems via optimization techniques and novel *green* technologies is both timely and essential.

Recently, ambient backscatter communications (AmBC) has emerged as a very promising low-energy technology [7, 8]. The backscatter device can transmit data in a passive way by recycling the radio frequency (RF) waves in the vicinity while harvesting energy. In the simplest implementation, the backscatter device, which consists of a dipole antenna, switches between two states: a backscattering state, in which the ambient signal coming from a source is reflected; and a transparent state, in which no signal is reflected. In practice, this is realized by setting the antenna to either a short or open circuit. These two states represent a binary code for its own message that can be decoded via a simple energy detector [7, 9, 10].

In this paper, our main objective is to investigate the energy-efficiency maximization in a multi-user downlink NOMA system that is aided by an ambient backscatter device.

A. Related works

Ambient backscatter communication systems have been widely investigated in the literature for OMA systems. In [11], the authors investigated the problem of signal detection of an ambient backscatter communication system composed

H. El Hassani and E. V. Belmega are with ETIS UMR 8051, CY Cergy Paris Université, ENSEA, CNRS, F-95000, Cergy, France (hajar.el-hassani@ensea.fr). A. Savard is with IMT Nord Europe, Institut Mines Télécom, Centre for Digital Systems, F-59653 Villeneuve d'Ascq, France and Univ. Lille, CNRS, Centrale Lille, UPHF, UMR 8520 - IEMN, F-59000 Lille, France. E. V. Belmega is also with Univ. Gustave Eiffel, CNRS, LIGM, F-77454, Marne-la-Vallée, France. R. C. de Lamare is with CETUC, PUC-Rio, Rio de Janeiro 22451-900, Brazil and the Dept. of Electronics, University of York, York, YO10 5DD, U.K.

A preliminary and special case of the work in this paper has been presented at IEEE GLOBECOM, Dec. 2021 [1].

This work has been supported by the ELIOT ANR-18-CE40-0030 and FAPESP 2018/12579-7, FAPERJ, CNPq and FAPESP projects and by IRCICA, CNRS USR 3380, Lille, France.

of a RF source and a backscatter device transmitting its binary signal to a receiver. The authors in [12] developed an optimal detector achieving a best detection performance and provided an analysis of the bit error rate (BER) and the outage probability performance. In a cooperative ambient backscatter communication system composed of a RF source and a backscatter transmitter who simultaneously send their messages to a receiver [13, 14], the ergodic rates upper bounds of both links were derived in [13] and an analysis of the achievable rate region of the system was done in [14]. For the same system model, the authors in [15] have analysed the error performance of an ambient backscatter device that uses an on-off keying modulation scheme (OOK) [7, 11, 16]. The exact analytical expressions of the average BER were derived under fading channels.

Several optimization problems were investigated in the context of backscatter communications considering either the simple backscattering state, or by making a simplifying approximation of the maximum achievable rate with Shannon capacity, without investigating the actual achievable information-theoretic rates when taking into account the backscatter device's message [17–19]. In [17], the ergodic capacity maximization of the backscatter-receiver link was investigated by jointly optimizing the transmit power of the source and the reflection coefficient of the backscatter device. In [18], an energy-efficient resource allocation scheme was proposed in terms of the optimal time allocation for the sleep vs. harvesting energy states of the backscatter device, its reflection coefficient, and the power of the RF source. Similarly, the authors in [19] have investigated the throughput maximization problem.

In the last years, a great research interest focused on investigating NOMA in the context of backscatter communications. The authors in [20], proposed a backscatter cooperation scheme for a two-user NOMA downlink system, where one of the users backscatters the surplus power of the received signal to enhance the reception of the other user. The outage performance, the ergodic rate, and the diversity-multiplexing trade-off (DMT) performance were analyzed. The optimal reflection coefficient and the optimal power allocation at the BS were derived under outage constraints for NOMA. In [21], an iterative algorithm for the optimal reflection coefficient and the power allocation policy was proposed to maximize the energy efficiency of a two-user downlink NOMA system aided by an ambient backscatter device. The authors in [22] considered the same model to enhance the sum rate of the system under imperfect SIC decoding. The same authors investigated the energy-efficiency maximization problem for a NOMA system aided by AmBC in a vehicular scenario under imperfect SIC decoding [23].

To sum up, the above relevant literature on NOMA systems aided by AmBC has covered both experimental and theoretical aspects. However, most of the existing works consider either the simple backscattering state only, or that the backscattered signal, which contains a multiplicative term of the ambient signal and the backscatter device message, has a Gaussian distribution, both cases leading to conventional Shannon capacity when deriving the achievable rates [13, 17–19, 21–24]. To the best of our knowledge, a rigorous investigation of the information-theoretic achievable rate regions of NOMA in the context of AmBC is still lacking. In this paper, we aim to fill this gap by first deriving the achievable rate regions and only then developing resource allocation techniques to optimize the energy efficiency of the system, in the general case in which the backscatter device sends its own independent information.

B. Our contributions

In our preliminary work [1], we derived the closed-form solution for the optimal reflection coefficient and the power allocation maximizing the energy efficiency of a multi-user NOMA system aided by AmBC, assuming that the backscatter device is constantly in a backscattering state, similarly to the aforementioned literature.

In contrast, in this paper, we investigate the general problem where the backscatter device also sends its own independent message to the users, for which the Shannon achievable rate region is unknown. The energy-efficiency objective is measured in terms of the tradeoff and the ratio between the sum rate and the power consumption. We consider minimum user rate and SIC decoding order constraints as well as a maximum power budget available at the transmitter.

Our main contributions in this paper are multi-fold:
i) First, we derive the information-theoretic achievable rate regions of a multi-receiver downlink NOMA system aided by an ambient backscatter device that reflects the signal coming from a source employing NOMA *while sending its own binary information*. Such a system is different from the conventional NOMA system because of the multiplicative operation at the backscatter device. Instead of considering the simple backscattering state or the approximation of the backscattered signal as a Gaussian distribution, we use an information-theoretic approach where we derive the achievable rate regions of the system for the general case of a discrete memoryless channel and the additive white Gaussian noise (AWGN) channel.
ii) We propose a joint optimization framework to maximize the energy efficiency of the NOMA-AmBC system, defined as the tradeoff and ratio between the sum rate and the power consumption. In particular, for an arbitrary number of receivers, and by assuming that the backscatter device data rate is much lower than that of the source, we jointly optimize the reflection coefficient and the power allocation under power budget, QoS, SIC decoding order and reflection coefficient constraints. The resulting optimization problem is not convex.
iii) To simplify this problem, we introduce a modification to the constraints. As a result, the problem can be decoupled and solved analytically (up to a line search) by first finding the optimal reflection coefficient, and then the optimal power allocation policy. We then show that our proposed optimal solution can reduce Dinkelbach's method to a line search when maximizing the ratio sum rate vs. power consumption.
iv) At last, our extensive numerical results demonstrate the negligible impact of the constraints modification on the optimality of our solution. The proposed solution is also shown to achieve higher energy efficiency than conventional NOMA and OMA (with and without backscattering). To complete our study, we also investigate the impact of imperfect channel state

information (CSI) on our solution and show its pertinence when the quality of the estimation is sufficient.

Notations: $\mathbb{I}(\cdot;\cdot)$, $\mathbb{H}(\cdot)$, $\mathbb{H}(\cdot,\cdot)$, $\mathbb{H}(\cdot|\cdot)$ denote the mutual information, entropy, joint and conditional entropy, respectively. $p(\cdot)$, $p(\cdot|\cdot)$ denote the probability mass function (pmf) and the conditional pmf. $C(\cdot) = \frac{1}{2}\log_2(1+\cdot)$ denotes the capacity of the AWGN channel. $\mathcal{N}(\cdot,\cdot)$ and $\mathrm{Bern}(\cdot)$ denote the normal and Bernoulli distribution. $\mathbb{P}(\mathcal{E})$ denotes the probability of the event $\mathcal{E}$. Vectors and scalars are denoted by bold and normal font letters. Random variables and their realizations are denoted by upper and lowercase letters, respectively.

II. System model

Consider an ambient backscatter multiple access downlink NOMA communication system depicted in Fig. 1 and composed of one transmitter or source (e.g., BS, femtocell, Wi-Fi hotspot, etc.) and $K \geq 2$ receivers or users (e.g., mobile phones, IoT devices, etc.), all equipped with a single antenna, and of an ambient backscatter device that can backscatter the RF signal coming from the source to send information and harvest energy. The source sends the message M_i encoded as the codeword X_i intended for each receiver $i \in \{1,\ldots,K\}$ with power p_i via *superposition coding* and broadcasts $X = \sum_{i=1}^{K} X_i$, which contains all the superimposed encoded messages. We assume that the backscatter device sends common information to all receivers.

Our system model has several practical applications such as: smart home, healthcare, and environmental monitoring. [9, 10, 17, 19, 25]. For example, in the smart home scenario, a Wi-Fi access point communicates with many smart phones while an IoT sensor – the backscatter device – in the home transmits its own low rate message (temperature, humidity, intruder motion measures, etc.) to the smart phones by riding on the existing Wi-Fi signals [16] and without any active RF chains.

The binary code B sent by the backscatter device to all receivers is encoded by modulating the amplitude of the direct signal with two distinct scattering states: an active backscattering state, in which the ambient signal is reflected and $B = 1$; and a transparent state, in which the backscatter device does not reflect the incoming signal and $B = 0$. Thus, the backscatter device can send information by switching between backscattering and transparent states, which is also called OOK and is commonly used in standardized backscatter devices due to its simplicity and ability to provide a higher energy harvesting rate than other schemes (e.g., binary phase-shift keying (BPSK)) [7, 11, 14, 16].

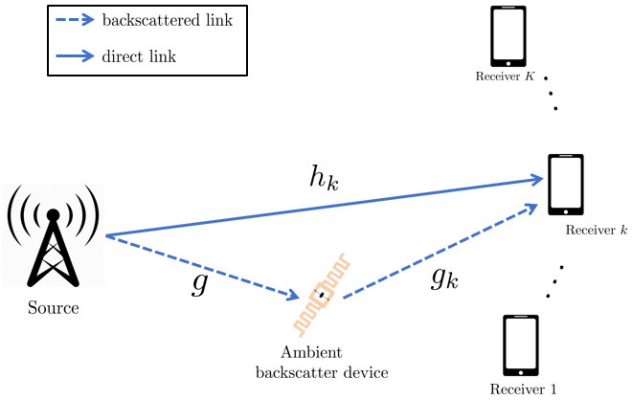

Fig. 1. Multi-user downlink NOMA system aided by an ambient backscatter device.

The received signal Y_k at user k is composed of the direct signal coming from the source and the backscattered signal, which is given by

$$Y_k = \underbrace{h_k X}_{\text{direct signal}} + \underbrace{\sqrt{\rho}\; g\; g_k B X}_{\text{backscattered signal}} + Z_k, \tag{1}$$

where h_k, g and g_k are the real[1] channel gains between the source and receiver k, the source and the backscatter device and the backscatter device and receiver k, respectively, $Z_k \sim \mathcal{N}(0,\sigma_k^2)$ is AWGN, and the parameter ρ is the reflection coefficient representing the percentage of the backscattered signal. The other portion $(1-\rho)$ of the signal is used for energy harvesting. Note that, in the transparent state $B = 0$, the backscatter device does not reflect the ambient signal, which is fully harvested for energy. Note that we do not consider explicitly the harvested energy at the backscatter device in our problem.[13, 20–23, 26].

Unless specified otherwise, we assume that perfect CSI is available at the source and that, without loss of generality, the channel gains h_k, $k \in \{1,\ldots,K\}$ are arranged in a decreasing order such that $h_k^2 \geq h_{k+1}^2, \forall k$ [3, 4]. This perfect CSI assumption is fairly common in the relevant literature [13, 17–19, 21, 22, 24, 27]. Nevertheless, we also investigate in Section V the effect of imperfect CSI on our proposed solution.

Following the superposition coding principle adopted in NOMA, each receiver i will perform SIC [3, 28] where it will first decode the messages of receivers with weaker channel gains X_j, $j \in \{K, K-1,\ldots,i+1\}$ (i.e., that are allocated more power by the source), while treating other messages X_s, $s \in \{j-1,\ldots,1\}$ as noise, before decoding its own message X_i. Note that the source decides the SIC ordering only based on the direct link to the users without accounting for the backscattered link. Indeed, since the backscatter device is inherently opportunistic when sending its own message, the source has no control over its backscattering state.

Unlike traditional wireless transmitters, the backscatter device does not possess power amplifiers and contains only passive components to perform low-power operations [7, 11–16]. Therefore, it is assumed that the data rate of the backscatter device is much lower than the data rate of the source. This is practically useful for receivers to separate the two signals through averaging using an energy detector when decoding the backscatter device message, where the performance depends on the difference in power between the backscattering and transparent states [7, 25]. We also assume that the signal processing delay and the noise at the backscatter device are negligible [7, 17].

Most of the existing works [13, 17–19, 21–24] consider either the simple backscattering state, or that the backscattered

[1]The full pathloss channel model is described in Section V. This assumption is justified in AmBC-enabled systems because of their small coverage region [20, 26, 27].

signal composed of the product $B\,X$ follows a Gaussian distribution where Shannon's information capacity expression $C(\cdot)$ is used to approximate the maximum achievable rate, without investigating the achievable rates when taking into account the backscatter device's message B. These assumptions may not be realistic in practice, since the backscatter device usually has its own information to transmit besides harvesting energy for its circuit operation. In the following, we take into account explicitly the message of the backscatter device, which clearly sets our work apart from the existing literature.

III. Information-theoretic achievable rate regions

Because of the multiplicative form of the backscattered signal $B\,X$ in the received signal Y_k in (1), where both X and B are random variables, the Shannon's capacity function $C(\cdot)$ cannot be applied to derive the achievable rates expressions. Hence, we start by deriving the information-theoretic achievable rate regions, before delving into resource optimization problems of the ambient backscatter NOMA system described previously.

A. General Case

Let us start with the *discrete memoryless channel* (DMC) case of the joint multiple access and broadcast communication system depicted in Fig. 2, and then derive the achievable rate region for the Gaussian channel described in our predefined model.

Both the source and the backscatter device wish to communicate independent messages reliably to K receivers. The backscatter device encodes its common message M_0 into a codeword B^n and transmits it over the shared channel. The source uses a superposition coding technique to encode each private message M_i destined to receiver i in a layered manner and broadcasts the codeword X^n consisting of all merged encoded messages $M_1,\ldots,M_K$. Upon receiving the sequence Y_i^n, receiver $i\in\{1,\ldots,K\}$ computes an estimate $\hat{M}_{0\to i}$ of the message M_0 and uses SIC to obtain an estimate $\hat{M}_{i\to i}$ of its message M_i, by first computing the estimates $\hat{M}_{j\to i}$ of the messages M_j, for all $j\in\{K,K-1,\ldots i+1\}$ following this precise successive order.

Using elements from information theory [29, 30], we first describe the codebook generation for both messages X, using the superposition coding technique, and B. We introduce the auxiliary random variables $U_j,\ j\in\{2,\ldots,K\}$ serving as "cloud centers" representing the messages M_j that can be distinguished by receivers $i\le j$. By defining the error events of unsuccessful decoding of X and B and by using typicality arguments, we derive the achievable rates for which the receivers can reliably decode X and B (i.e., when the average probability of error $\mathbb{P}(\varepsilon_i)$ of each receiver i tends to 0). Complete details can be found in Appendix A. The resulting achievable rate region of the ambient backscatter NOMA system is given in the following theorem.

Theorem 1. *The achievable rate region of the discrete memoryless source-backscatter device to K receivers channel is given by the set of rate tuples $(R_0,R_1,\ldots,R_K)$ defined below*

$$\begin{aligned}
R_0 &\le \min_{1\le i\le K}\mathbb{I}(B;Y_i|U_K), &(2)\\
R_K &\le \min_{1\le i\le K}\mathbb{I}(U_K;Y_i|B), &(3)\\
R_0+R_K &\le \min_{1\le i\le K}\mathbb{I}(U_K,B;Y_i), &(4)\\
R_j &\le \min_{i\le j}\mathbb{I}(U_j;Y_i|B,U_K,\ldots,U_{j+1}),\forall\,1\le j\le K-1, &(5)
\end{aligned}$$

where U_i are auxiliary randoms variables accounting for X_i for all $2\le i\le K$.

In practice, the data rate of the backscatter device is significantly lower than that of the source because of its design simplicity and power limitations, as also argued in [7, 11–16]. Assuming that $R_0\ll R_K$ in particular, the expressions in (3) and (4) in Theorem 1 reduce to

$$\begin{aligned}
R_K &\le \min\left(\min_{1\le i\le K}\mathbb{I}(U_K;Y_i|B),\min_{1\le i\le K}\mathbb{I}(U_K,B;Y_i)\right) &(6)\\
&\overset{(a)}{=} \min_{1\le i\le K}\mathbb{I}(U_K;Y_i|B), &(7)
\end{aligned}$$

where (a) follows from the chain rule and the positivity of the mutual information. This yields the achievable rate region given in the following Lemma.

Lemma 1. *Assuming that the backscatter device has a very low data rate compared to that of the source, $R_0\ll R_K$, the achievable rate region in Theorem. 1 simplifies to*

$$\begin{aligned}
R_0 &\le \min_{1\le i\le K}\mathbb{I}(B;Y_i|U_K), &(8)\\
R_K &\le \min_{1\le i\le K}\mathbb{I}(U_K;Y_i|B), &(9)\\
R_j &\le \min_{i\le j}\mathbb{I}(U_j;Y_i|B,U_K,\ldots,U_{j+1}),\ \forall 1\le j\le K-1. &(10)
\end{aligned}$$

B. Gaussian Channels

Having obtained the achievable rate region in the discrete memoryless case given in Lemma 1, we now derive the achievable rate region for the AWGN model described in Section II and, more specifically, for the received signal Y_k observed at each receiver k and given in (1).

We assume that the message of the backscatter device B follows the Bernoulli distribution $B\sim\mathrm{Bern}(q)$, where $q=\mathbb{P}(B=1)$ is the probability of the backscattering state and $(1-q)=\mathbb{P}(B=0)$ is the probability of the transparent state. By assuming that $V\sim\mathcal{N}(0,p_1)$ and $U_i\sim\mathcal{N}(0,p_i),\forall i\in\{2,\ldots,K\}$, which stand for X_1 and $X_i,\forall i\in\{2,\ldots,K\}$, respectively, that are most commonly used in the NOMA literature when describing the sent codeword $X=\sum_{k=i}^{K}X_i$, we can compute the achievable rate region for the Gaussian case.

Theorem 2. *Assuming that the backscatter device has a very low data rate compared to that of the source, $R_0\ll R_K$, the achievable rate region of the AWGN source-backscatter device to K-receiver channel is the set of rate tuples $(R_0,R_1,\ldots,R_K)$, such that*

$$\begin{aligned}
R_0 \le \min_{1\le i\le K}\mathbb{H}(Y_i|U_K) &-\frac{q}{2}\log_2\left(2\pi e\sigma_i^2\left(H_{i|1}(\rho)\sum_{k=1}^{K-1}p_k+1\right)\right)\\
&-\frac{1-q}{2}\log_2\left(2\pi e\sigma_i^2\left(H_{i|0}\sum_{k=1}^{K-1}p_k+1\right)\right),
\end{aligned}$$

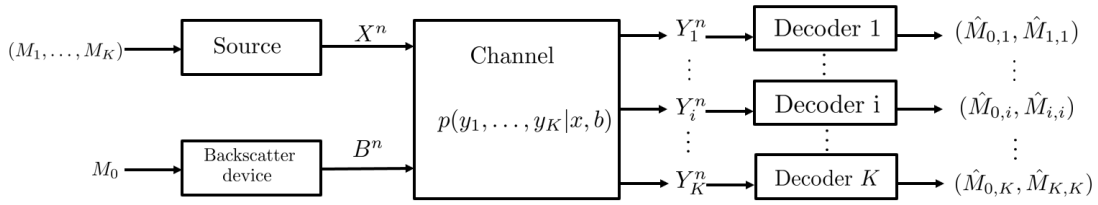

Fig. 2. Source-backscatter device to K-receivers discrete channel model

$$R_k \leq qC\left(\min_{i\leq k}(\gamma_{k\to i|1})\right)+(1-q)C\left(\min_{i\leq k}(\gamma_{k\to i|0})\right),$$
$$\forall\ 1\leq k\leq K,$$

where $H_{i|0}=h_i^2/\sigma_i^2$, $H_{i|1}(\rho)=(h_i+\sqrt{\rho}gg_i)^2/\sigma_i^2$ represent the channel gains normalized by the noise variance when the backscatter device is in the transparent state ($B=0$) and in the backscattering state ($B=1$), respectively, and $\gamma_{k\to i|0}=\frac{H_{i|0}p_k}{1+H_{i|0}(p_1+\ldots+p_{k-1})}$ and $\gamma_{k\to i|1}=\frac{H_{i|1}(\rho)p_k}{1+H_{i|1}(\rho)(p_1+\ldots+p_{k-1})}$ are the corresponding signal-to-interference-plus-noise ratio (SINR) values when receiver i decodes the message intended for receiver k.

Above, we provide the expressions of the achievable rates of the backscatter and of the receivers in the Gaussian case. Note that the expression of R_0 cannot be obtained in closed form because of the first term on the right hand side. Also, the achievable rate of receiver k can be seen as an expected value of the Shannon capacity over the message $B\in\{0,1\}$ (i.e., the ergodic rate over the fading channel $h_k+\sqrt{\rho}gg_kB$).

The proof of Theorem 2 exploits information-theoretic techniques where the continuous random variables $V\sim\mathcal{N}(0,p_1)$ and $U_k\sim\mathcal{N}(0,p_k)$ are quantized to extend the expressions of mutual information in the DMC given in Lemma 1 to the Gaussian channel [29, 30]. The Gaussian distribution is chosen such that it maximizes the mutual information expressions in (9) and (10). [2] The complete details are provided in Appendix A. At last, note that the conditional entropy term $\mathbb{H}(Y_i|U_K)$ in Theorem 2 is very difficult to compute in closed form because of the non trivial sum of two dependent variables X and B X in the received signal Y_k, where $B\sim\text{Bern(p)}$ and $X\sim\mathcal{N}(0,\sum_{i=1}^K p_i)$, and is left open for future investigation.

Having derived the achievable rate regions for our system model described in Section II, we now investigate the energy-efficiency maximization problem. Since by assumption we have $R_0\ll R_K$, and knowing that the backscatter device is a low-power device that performs energy harvesting for its own circuit operations, we only focus on maximizing the energy efficiency of the downlink NOMA system (aided by ambient backscattering).

IV. Energy-efficiency maximization problem

In this section, we formulate the energy efficiency optimization of the NOMA downlink system in the presence of an ambient backscatter device as a tradeoff between the sum rate of receivers and the total power consumption [31, 32].

[2]Note that the Gaussian assumption is optimal for the source assuming $R_0\ll R_K$, but may not be optimal in general.

A. Problem formulation

The above leads to the following optimization problem

$$(\mathbf{EE0})\quad \max_{(\rho,\mathbf{p})\in\mathcal{P}}\sum_{k=1}^K R_k(\rho,\mathbf{p})-\alpha\left(\sum_{k=1}^K p_k+P_c\right), \quad (11)$$

where $R_k(\rho,\mathbf{p})$ denotes the achievable rate of receiver k[3] and follows from Theorem 2

$$R_k(\rho,\mathbf{p})=qC\left(\min_{i\leq k}(\gamma_{k\to i|1})\right)+(1-q)C\left(\min_{i\leq k}(\gamma_{k\to i|0})\right),$$
$$\forall\ 1\leq k\leq K, \quad (12)$$

and P_c is the circuit power. The weighting parameter $\alpha>0$ in the objective captures the tradeoff between the sum of achievable rates and the consumed power similarly to [1, 5, 32], where larger values of α favor the maximization of the achievable sum rate, while smaller values of α favor the minimization of the power consumption.

The set $\mathcal{P}$ contains all admissible reflection coefficients ρ and transmit power allocation policies $\mathbf{p}=(p_1,\ldots,p_K)$. This feasible set accounts for all the constraints: the maximum power budget of the source, the receivers's targeted quality of service (QoS) expressed as $R_k(\rho,\mathbf{p})\geq R_{\min,k}$, the successful SIC process expressed as $qC\left(\gamma_{k\to i|1}\right)+(1-q)C\left(\gamma_{k\to i|0}\right)\geq qC\left(\gamma_{k\to k|1}\right)+(1-q)C\left(\gamma_{k\to k|0}\right)$ to avoid error propagation when receiver i, $\forall i\leq k-1$, performs SIC and decodes the message destined to receiver k, and the range of the reflection coefficient, respectively. Note that when $q=0$ and $q=1$, i.e., pure transparent state and pure backscattering state, the optimization problem ($\mathbf{EE0}$) is equivalent to the optimization problem solved in our previous work [5] and [1], respectively.

Since SIC decoding is a key component for NOMA [3, 22, 28, 33], it has to be performed successfully and independently from the backscatter device's state (backscattering or transparent) in order to avoid error propagation that may affect the performance of the system (e.g., the targeted quality of service). To ensure successful SIC, we impose the minimum QoS constraint, in terms of the minimum SINR level, on each state of the backscatter device: $\gamma_{k\to i|1}\geq\gamma_{k\to k|1}$ for the backscattering state ($q=1$), and $\gamma_{k\to i|0}\geq\gamma_{k\to k|0}$ for the

[3]Note that this achievable rate can be seen as an expected value of the achievable rate over the message $B\in\{0,1\}$ (i.e., the ergodic rate over the fading channel $h_k+\sqrt{\rho}gg_kB$).

transparent state ($q=0$), $\forall k \in \{1,\dots,K\}$ and $i \le k$. All the above leads to the feasible set

$$\mathcal{P} \triangleq \Bigg\{ (\rho,\mathbf{p}) \in [0,1]\times\mathbb{R}_+^K \;\Bigg|\; 0\le\rho\le 1, \sum_{j=1}^{K} p_j \le P_{\max}, \; R_k(\rho,\mathbf{p}) \ge R_{\min,k}, \gamma_{k\to i|0} \ge \gamma_{k\to k|0}, \gamma_{k\to i|1} \ge \gamma_{k\to k|1}, \; \forall 1\le k\le K, \forall i\le k \Bigg\}. \quad (13)$$

Note that the successful SIC decoding constraint in the transparent state, given as $\gamma_{k\to i|0} \ge \gamma_{k\to k|0}$, is equivalent to $\frac{p_k}{\frac{1}{H_{i|0}}+(p_1+\dots+p_{k-1})} \ge \frac{p_k}{\frac{1}{H_{k|0}}+(p_1+\dots+p_{k-1})}$, which is readily satisfied due to the assumed channels ordering (i.e. $H_{i|0}=h_i^2/\sigma_i^2 \ge H_{k|0}=h_k^2/\sigma_k^2, \quad \forall k\ge 2, i\le k-1$), and can hence be removed altogether. Second, since the successful SIC constraint in the transparent state $\gamma_{k\to i|0} \ge \gamma_{k\to k|0}$ is readily satisfied, and by ensuring that $\gamma_{k\to i|1} \ge \gamma_{k\to k|1}, \forall i \le k$ is met in the optimization problem ($\mathbf{EE0}$), the achievable rate of receiver k in (12) reduces to

$$R_k(\rho,\mathbf{p}) = qC(\gamma_{k\to k|1}) + (1-q)C(\gamma_{k\to k|0}), \; \forall\, 1\le k\le K. \quad (14)$$

To simplify the presentation and the mathematical derivations henceforth, we introduce the notations $\theta_k(\mathbf{p}) = \sum_{i=1}^{k} p_i$, $\forall 1\le k\le K$ with $\theta_0(\mathbf{p})=0$. Using these notations and all the above considerations, our optimization problem is equivalent to

$$\begin{aligned}
(\mathbf{EE0}) \quad & \max_{\rho,\mathbf{p}} \sum_{k=1}^{K} R_k(\rho,\mathbf{p}) - \alpha(\theta_K(\mathbf{p})+P_{\rm c}) \\
\text{s.t. } & \theta_K(\mathbf{p}) \le P_{\max}, && (C1)\\
& R_k(\rho,\mathbf{p}) \ge R_{\min,k}, \quad \forall\, 1\le k\le K && (C2)\\
& \gamma_{k\to i|1}(\rho,\mathbf{p}) \ge \gamma_{k\to k|1}(\rho,\mathbf{p}), \\
& \quad \forall\, 2\le k\le K, \forall\, i\le k-1 && (C3)\\
& 0\le\rho\le 1. && (C4)
\end{aligned}$$

Now, a major issue in the above optimization problem is the minimum rate constraint $(C2)$ which makes ($\mathbf{EE0}$) non-convex. Indeed, the rate $R_k(\rho,\mathbf{p})$ is not concave w.r.t. $\mathbf{p}$ since $R_k(\rho,\mathbf{p})$ is expressed as a weighted sum of the capacity in the backscattering state $C(\gamma_{k\to k|1})$ and the capacity in the transparent state $C(\gamma_{k\to k|0})$.

To overcome this challenge, we introduce a modification to this constraint as follows: instead of having $R_k(\rho,\mathbf{p}) \ge R_{\min,k}$, we require each of the averaged terms in (14) to be bounded: $C(\gamma_{k\to k|0}) \ge R_{\min,k}$ and $C(\gamma_{k\to k|1}) \ge R_{\min,k}$. This means that the QoS constraint needs to be satisfied in the transparent state and in the backscattering state individually. This modification restricts in fact the original feasible set, leading to a potential optimality loss in case the optimal solution of ($\mathbf{EE0}$) lies outside of the restricted constraints. In our setting, we believe that any incurred optimality loss will be limited. This intuition, validated through numerical results in Section V, is based on the the fact that the rate of the backscatter device is much lower than that of the source in practice. This implies that the message of the backscatter remains fixed for a relatively long period of time from the source's perspective and, hence, imposing the minimum source rate constraint for each individual backscatter state is relevant.

By imposing the QoS constraints on each state separately, and after some mathematical manipulations, the constraint $(C2)$ can be expressed as

$$\theta_k(\mathbf{p}) \ge A_k\theta_{k-1}(\mathbf{p}) + \frac{A_k-1}{H_{k|0}}, \quad \forall\, k\le K, \forall i\le k-1, \quad (15)$$

$$\theta_k(\mathbf{p}) \ge A_k\theta_{k-1}(\mathbf{p}) + \frac{A_k-1}{H_{k|1}(\rho)}, \quad \forall\, k\le K, \forall i\le k-1, \quad (16)$$

where $A_k = 2^{2R_{\min,k}}$. The main advantage of this modification is that it leads to the following simpler non-convex optimization problem, which we show can be solved analytically.

$$\begin{aligned}
(\mathbf{EE1}) \quad & \max_{\rho,\mathbf{p}} \sum_{k=1}^{K} R_k(\rho,\mathbf{p}) - \alpha(\theta_K(\mathbf{p})+P_{\rm c}) \\
\text{s.t. } & \theta_K(\mathbf{p}) \le P_{\max}, && (C1)\\
& \theta_k(\mathbf{p}) \ge A_k\theta_{k-1}(\mathbf{p}) + \frac{A_k-1}{H_{k|0}}, \\
& \quad \forall\, 2\le k\le K, \forall\, i\le k-1 && (C2a)\\
& \theta_k(\mathbf{p}) \ge A_k\theta_{k-1}(\mathbf{p}) + \frac{A_k-1}{H_{k|1}(\rho)}, \\
& \quad \forall\, 2\le k\le K, \forall\, i\le k-1 && (C2b)\\
& \frac{p_k}{\frac{1}{H_{i|1}(\rho)}+\theta_{k-1}(\mathbf{p})} \ge \frac{p_k}{\frac{1}{H_{k|1}(\rho)}+\theta_{k-1}(\mathbf{p})}, \\
& \quad \forall\, 2\le k\le K, \forall\, i\le k-1 && (C3)\\
& 0\le\rho\le 1, && (C4)
\end{aligned}$$

where $(C2a)$ and $(C2b)$ are the modified QoS constraints for the transparent and backscattering states, respectively, and all other constraints remain unchanged. Note that since $H_{k|1}(\rho) \ge H_{k|0}$ ($H_{k|1}(\rho)$ is a composition of the direct and backscattered channels), the constraint $(C2b)$ will be omitted since satisfying $(C2a)$ is sufficient.

Even though we restricted $(C2)$ to simplify the problem ($\mathbf{EE0}$), the resulting optimization problem ($\mathbf{EE1}$) remains non-convex due to the joint optimization of the reflection coefficient ρ and the vector of allocated powers $\mathbf{p}$. Nevertheless, following a similar approach to [1] (in which the backscatter device did not transmit any information and operated always a in backscattering state), we show here that ($\mathbf{EE1}$) can be solved by decoupling it into two sub-problems without loss of optimality: i) we first optimize ρ for an arbitrary power allocation $\mathbf{p}$; ii) then optimize $\mathbf{p}$ with the fixed optimal reflection coefficient ρ^*.

B. Optimal reflection coefficient

Let us first consider a fixed arbitrary power allocation $\mathbf{p}\in\mathcal{P}$ and solve the optimization problem ($\mathbf{EE1}$) w.r.t. to the reflection coefficient ρ. It turns out that the optimal reflection coefficient is independent of $\mathbf{p}$ and can be obtained in closed form

$$\rho^* = \begin{cases} \min\left(1, \min\xi\right), & \text{if } \; \xi\neq\emptyset \\ 1, & \text{otherwise,} \end{cases} \quad (17)$$

where $\xi \triangleq \left\{ \left(\frac{h_k}{\sigma_k}-\frac{h_{k+1}}{\sigma_{k+1}}\right)^2 \Big/ \left(g(\frac{g_{k+1}}{\sigma_{k+1}}-\frac{g_k}{\sigma_k})\right)^2 \;\middle|\; 2\le k\le K, h\text{s.t. } g_{k+1}>g_k \right.$
The proof follows similarly to our previous work [1].

Given the optimal reflection coefficient ρ^* in (17), the constraints $(C3)$ and $(C4)$ are readily satisfied since, as proven in [1], it leads to $H_{i|1}(\rho^*) \geq H_{k|1}(\rho^*), \forall i \leq k-1$, and in particular $H_{1|1}(\rho^*) \geq \ldots \geq H_{K|1}(\rho^*)$. This will be very useful when deriving the optimal power allocation vector $\mathbf{p}^*$. Since the optimal reflection coefficient ρ^* in (17) is independent of $\mathbf{p}$ and the remaining constraints $(C1)$ and $(C2a)$ are independent of ρ, decoupling the optimization problem by first optimizing over the reflection coefficient and then over the power allocation policy does not induce any optimality loss.

C. Optimal power allocation

We can thus fix $\rho = \rho^*$ given in (17) and solve the remaining optimization problem, where $(\mathbf{EE1})$ reduces to $(\mathbf{EE2})$ below, in terms of the power allocation policy $\mathbf{p}$ with no optimality loss.

$$(\mathbf{EE2}) \quad \max_{\mathbf{p}} \ \eta_{EE}(\mathbf{p}) \triangleq \sum_{k=1}^{K} R_k(\rho^*, \mathbf{p}) - \alpha(\theta_K(\mathbf{p}) + P_{\mathrm{c}})$$

$$\text{s.t. } \theta_K(\mathbf{p}) \leq P_{\max}, \qquad (C1)$$

$$\theta_k(\mathbf{p}) \geq A_k \theta_{k-1}(\mathbf{p}) + \frac{A_k - 1}{H_{k|0}}, \quad \forall\ 1 \leq k \leq K. \qquad (C2a)$$

The remaining problem above is a convex optimization one since the objective function is concave w.r.t. $\mathbf{p}$, as shown in Appendix B, and the constraints $(C1)$ and $(C2a)$ are affine.

Feasibility condition: Because of the QoS requirements of each receiver, the convex optimization problem $(\mathbf{EE2})$ may not be feasible. Indeed, the power budget at the source $P_{\max}$ has to be greater or equal to the minimum power needed for satisfying the receiver's QoS constraints in $(C2a)$, expressed as $P_{\min} \triangleq \sum_{i=1}^{K} \frac{(A_i-1)}{H_{i|0}} \prod_{j=i+1}^{K} A_j \leq P_{\max}$, which follows similarly as in our previous work on optimal power allocation policies for K-receivers downlink NOMA without the backscatter device [5].

If the aforementioned feasibility condition is met, and given that $(\mathbf{EE2})$ is convex, we can apply the Lagrange multipliers to obtain the optimal expressions of $p_k^*,\ \forall k \geq 2$ as functions of p_1 by solving the Karush-Kuhn-Tucker (KKT) optimality conditions, which are necessary and sufficient [34]. Hence, as proven in Appendix B, the multi-variable problem $(\mathbf{EE2})$ is turned into a single variable optimization problem w.r.t. p_1 (which is proven to be a convex optimization problem), leading to our main result below.

Theorem 3. *If the optimization problem* $(\mathbf{EE2})$ *is feasible, the optimal power allocation* $\mathbf{p}$ *is given analytically as follows:*

$$\begin{aligned} p_k^*(\alpha) &= (A_k - 1)\left(\frac{1}{H_{k|0}} + p_1^* \prod_{i=2}^{k-1} A_i \right. \\ &\quad \left. + \sum_{i=2}^{k-1} \frac{(A_i - 1)}{H_{i|0}} \prod_{j=i+1}^{k-1} A_j\right), \quad \forall\ k \geq 2, \\ p_1^*(\alpha) &= \max\left(\min\left(\overline{p_1}(\alpha); u\right); \ell\right), \end{aligned}$$

where $\ell = \frac{(A_1-1)}{H_{1|0}}$, $u = \left(P_{\max} - P_{\min} + \ell \prod_{j=2}^{K} A_j\right) \Big/ \prod_{i=2}^{K} A_i$ *and* $\overline{p_1}(\alpha)$ *represents the unique critical point of the single variable function* $f_1(p_1) \triangleq \eta_{EE}(p_1, p_2^*, \ldots, p_K^*)$ *w.r.t.* p_1.

Unlike our previous works [5] and [1], since the backscatter device sends its own message, the resulting achievable rate expressions are significantly more complex and lead to a more technically involved solution. The proof is detailed in Appendix B.

In conclusion, in equation (17) and Theorem 3 we provide a closed-form expression for the optimal backscattering reflection coefficient and an almost closed-form expression for the optimal power allocation vector, respectively, thanks to our modified constraints in $(\mathbf{EE1})$. Indeed, to compute the optimal power allocation vector we only need to compute numerically the critical point $\overline{p_1}(\alpha)$ via a single line search. Our solution is hence scalable and of low complexity as only one line search is needed irrespective from the problem dimension. At the opposite, the brute force benchmark, illustrated in the numerical section for comparison purpose, has an exponential complexity with the problem dimension.

D. Energy efficiency as the ratio sum rate vs. overall consumed power

We investigate here a well-known energy-efficiency metric defined as the ratio between the achievable sum rate and the overall consumed power: $\xi_{EE}(\rho, \mathbf{p}) = \frac{\sum_{k=1}^{K} R_k(\rho, \mathbf{p})}{\sum_{k=1}^{K} p_k + P_c}$ [31] which can also be maximized by exploiting our optimal solution $(\rho^*, \mathbf{p}^*)$ of $(\mathbf{EE1})$.

Since only the numerator (the sum of achievable rates) depends on the reflection coefficient ρ, the optimal ρ^* given in (17) also maximizes $\xi_{EE}(\rho, \mathbf{p})$ for all feasible $\mathbf{p}$. Once ρ^* obtained, the energy-efficiency ratio $\xi_{EE}(\rho^*, \mathbf{p})$ becomes a fractional program, because the numerator $\sum_{k=1}^{K} R_k(\rho^*, \mathbf{p})$ is concave w.r.t. $\mathbf{p}$ (as shown in Appendix B) and the denominator $\sum_{k=1}^{K} p_k + P_c$ is affine. This fractional program can be solved using Dinkelbach's method [31], which reduces to finding the solution to the following equation w.r.t. α

$$F(\alpha) \triangleq \sum_{k=1}^{K} R_k(\rho^*, \mathbf{p}^*) - \alpha \left(\sum_{k=1}^{K} p_k^* + P_c\right) = 0, \qquad (18)$$

where $\mathbf{p}^*$ is given in Theorem 3 and which depends implicitly on α.

V. Numerical simulations

In this section, we present and discuss numerical results to evaluate the performance of our energy-efficient solution. For this, we consider the following scenario: the positions of the users are uniformly drawn in a disk of radius 20 m around the source. Similarly, the backscatter device position is drawn in a disk of radius 4 m surrounding the source. Since the coverage area of ambient backscatter communication systems is relatively small, we assume that the communication links have a strong line-of-sight (LOS) and fading-free pathloss channels of the type $h = d^{-\frac{\gamma}{2}}$ [20, 27], where d is the distance between different nodes and γ is the path loss exponent.

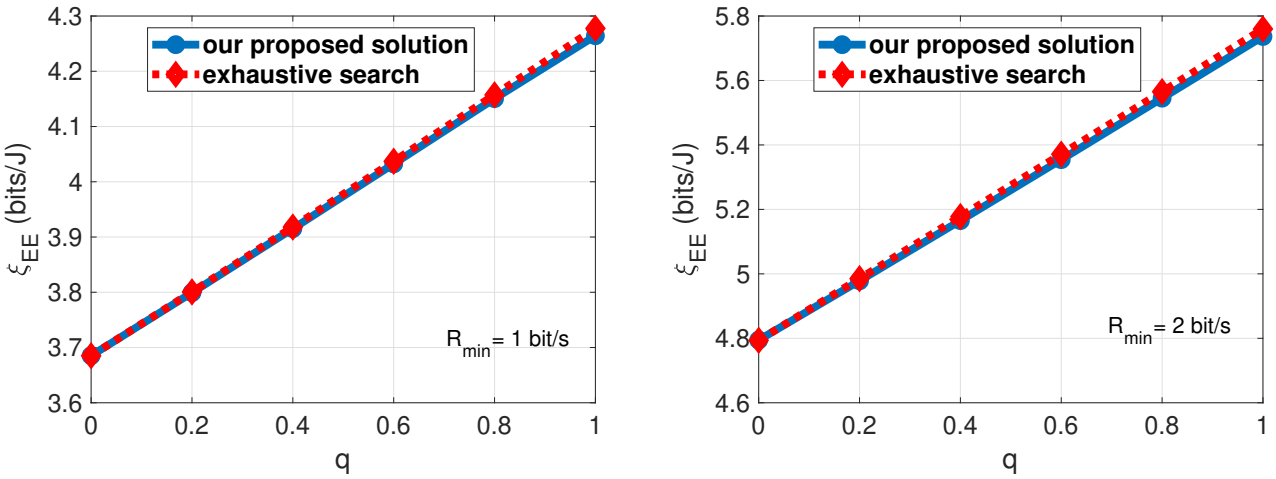

Fig. 3. Energy efficiency (ξ_{EE}) sub-optimality comparison for different values of q and $R_{\min}$.

Parameter	Value
Channel realizations	10^3
γ	2.5
$\sigma_k^2 = \sigma^2$	-20 dBm
$R_{\min,k} = R_{\min}$	1 bit/channel use (bpcu)
$P_{\max}$	30 dBm
P_c	30 dBm

TABLE I
SIMULATION PARAMETERS

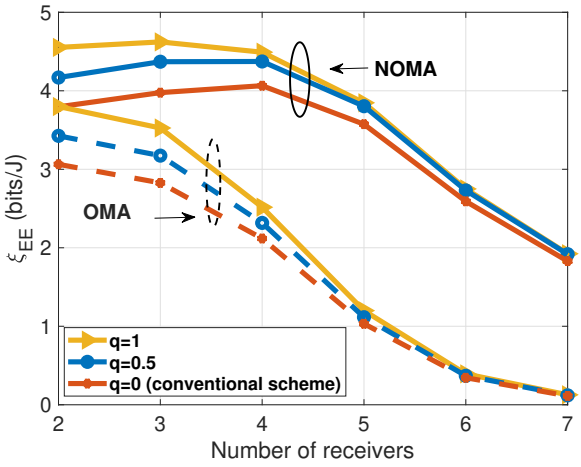

Fig. 4. Energy efficiency (ξ_{EE}) as a function of the number of receivers K for different values of q.

The system parameters are summarized in Table I unless stated otherwise. The simulation results are averaged over 10^3 random draws of the nodes positions satisfying the feasibility condition in Section IV-C.

Impact of our modified constraints: In Fig. 3, we compare the energy efficiency of the optimal solution to the original problem (**EE0**), obtained via exhaustive search[4], and our analytical solution to the modified problem (**EE1**) as a function of $q \in [0, 1]$ and for $R_{\min} \in \{1, 2\}$ bpcu. We see that the sub-optimality gap becomes smaller when q decreases since the feasible set of (**EE1**) becomes less and less restricted until becoming identical to the feasible set of (**EE1**), implying that the optimal solution of the modified problem (**EE1**) coincides with the optimal solution of the original problem (**EE0**). Indeed, the case $q = 0$ corresponds to conventional NOMA, without backscattering, for which the two solutions are identical, as (**EE0**) becomes equivalent to (**EE1**). The sub-optimality gap increases with $R_{\min}$, but remains negligible, which validates our intuition and highlights the interest of our analytical solution.

NOMA vs. OMA evaluation: In Fig. 4, we plot the energy efficiency ξ_{EE} of ambient backscatter-aided NOMA and OMA (as a benchmark), as a function of the number of receivers for different values of $q \in \{0, 0.5, 1\}$ with $P_{\max} = 60$ dBm and $R_{\min} = 1$ bpcu. For a fair comparison, we consider OMA with equal time sharing slots among the users, and for which we can show that the optimal $\rho^{*,\mathrm{OMA}} = 1$ and we can find analytically the optimal power allocation policy $\mathbf{p}^{*,\mathrm{OMA}}$ (which we omit here because of space limitations).

First, we see that NOMA with backscattering always outperforms its OMA counterpart irrespective of q. Moreover, we observe that the energy efficiency decreases with the number of receivers. The intuition comes from the expression of the optimal reflection coefficient in (17) that depends on the smallest difference between the channel gains. The larger the number of receivers K, the smaller the channel gap. When K increases, ρ^* tends to zero, vanishing the backscattering effect and leading to the conventional scheme without backscattering ($q = 0$).

In Fig. 5 we plot the achievable sum rate and overall power consumption as a function of the tradeoff parameter α where $q = 0.5$ and $R_{\min} = 1$ bpcu. We see that NOMA achieves a higher sum rate while consuming as much power as OMA, irrespective of α. Moreover, both the sum rate and power consumption decrease as α grows larger. Indeed, for larger values of α, the power minimization is given more weight when maximizing the sum rate vs. power consumption tradeoff. We

[4]The grid quantization step for every control variable is set to 10^{-3} in the exhaustive search procedure.

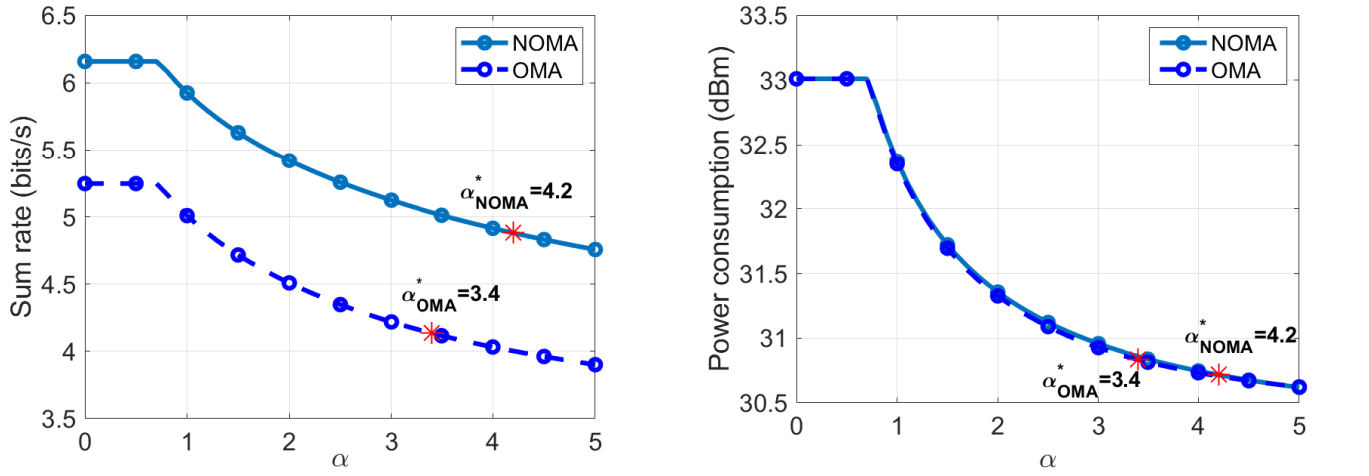

(a) Achievable sum rate.

(b) Overall power consumption.

Fig. 5. Achievable sum rate and overall power consumption as functions of the tradeoff parameter α for an ambient backscatter-aided NOMA system with $K = 2$ and $q = 0.5$.

also highlight the two points α^*_{NOMA} and α^*_{OMA} referring to the respective solutions of $F(\alpha) = 0$ in (18) providing the achievable sum rate and overall power consumption that are optimal in the sense of the energy-efficiency ratio ξ_{EE}.

Impact of imperfect CSI: At last, we investigate the impact of imperfect CSI on our solution. We assume that only channel gain estimates $\hat{h}$ are available at the transmitter side, such that $\hat{h} = h - e$, where $e \sim \mathcal{N}(0, \sigma_e^2)$ represents the estimation error of variance σ_e^2 for any link h. The power allocation policy is computed based on the estimated channel gains $\hat{h}$ and the system performance is obtained with the true channel gains h. Imperfect CSI may result in violating the user QoS constraints or the SIC constraints in (13), leading to an outage event. Hence, we plot in Fig. 6 both the energy efficiency when the system is not in outage and the outage probability for $q = 0.5$.

As expected, the performance is impacted by the quality of the channel estimation. For $\sigma_h^2/\sigma_e^2 \in \{-10, -20\}$ dB (poor estimation), the system is almost always in outage. For $\sigma_h^2/\sigma_e^2 = 20$ dB (excellent estimation) the imperfect CSI curves are superposed to the perfect CSI ones. When $\sigma_h^2/\sigma_e^2 = 10$ dB (good estimation), the outage is negligible and the energy efficiency is impacted but not critically so (the loss is below 11% for any K). When the error variance is as high as the channel variance ($\sigma_h^2/\sigma_e^2 = 0$ dB), the outage is very high: above 50% for $K = 2$ and reaches up to 90% for $K = 7$. Except for $K = 2$, the energy efficiency is also highly impacted in this case, with the loss reaching up to 49% for $K = 7$ users. Hence, our solution relies on high quality CSI estimation. When this is unavailable, the impact of CSI errors has to be taken into account in the problem formulation and the solution design.

VI. Conclusions and Perspectives

In this paper, we analyzed a multi-user downlink NOMA system aided by an ambient backscatter device. We first derived the information-theoretic achievable rate regions and then we formulated the energy efficiency maximization as the tradeoff between the sum rate and the power consumption. By introducing a modification to the problem's constraints, we simplified the non-convex optimization problem, which allowed us to obtain an analytical solution for the joint optimal reflection coefficient and power allocation policy (up to a line search). Our simulation results showed the negligible impact on the sub-optimality gap resulting from our modification. Moreover, the ambient backscatter-aided NOMA system was shown to outperform conventional NOMA and OMA (with and without backscattering) as benchmarks. Finally, we investigated the impact of imperfect CSI and highlighted that when the channel estimation is sufficiently high (SNR higher than 10 dB) our solution is still relevant. In highly dynamic systems or whenever the channel estimation is too poor, other solutions have to be investigated based on robust optimization or adaptive machine learning techniques, which represents an interesting future research perspective. Other future directions could be incorporating more realistic circuit and processing power consumption considerations as well as extending the investigation to consider imperfect CSI in the problem formulation.

Appendix A
Information-Theoretic Achievable Rate Regions

A. Proof of Theorem 1 (discrete memoryless channels)

First, we have to introduce the proper information-theoretic definitions needed for the coding and decoding procedures. We consider a two-sender K-receiver discrete memoryless channel defined by the tuple $(\mathcal{X} \times \mathcal{B}, p(y_1, \ldots, y_K|x, b), \mathcal{Y}_1 \times \ldots \times \mathcal{Y}_K)$ that consists of $K + 2$ finite sets: $\mathcal{X}$, $\mathcal{B}$, $\mathcal{Y}_1, \ldots, \mathcal{Y}_K$ and a collection of conditional probability mass functions (pmfs) $p(y_1, \ldots, y_2|x, b)$ defined on $\mathcal{Y}_1 \times \ldots \times \mathcal{Y}_K$. A $(2^{nR_0}, 2^{nR_1}, \ldots, 2^{nR_K}, n)$ code consists of:

- $K + 1$ message sets $[1 : 2^{nR_0}]$, $[1 : 2^{nR_1}], \ldots, [1 : 2^{nR_K}]$,
- two encoders, where encoder 1, the source, assigns a codeword $x^n(m_1, \ldots, m_K)$ to each message

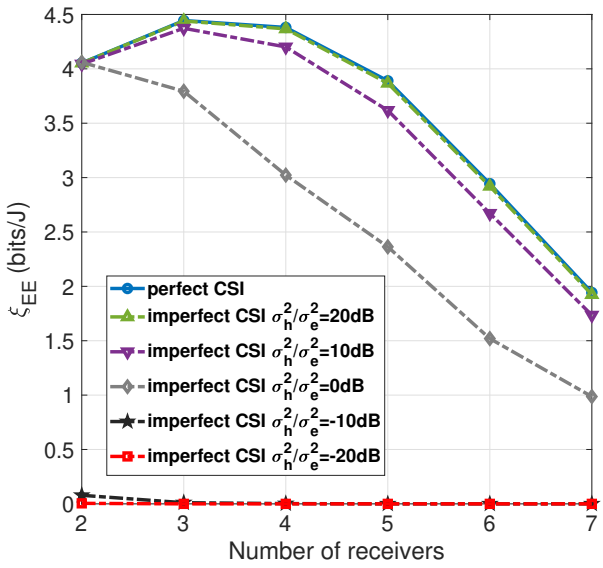

(a) Energy efficiency (ξ_{EE}) for different values of σ_e^2.

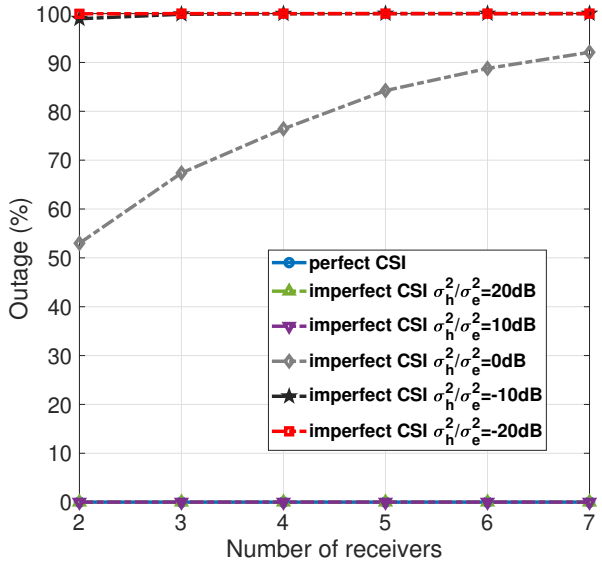

(b) Outage performance for different values of σ_e^2.

Fig. 6. Impact of imperfect CSI on the energy efficiency (ξ_{EE}) and outage performance of NOMA as a function of the number of receivers K for different values of the error variance σ_e^2.

$(m_1, \ldots, m_K) \in [1 : 2^{nR_1}] \times \ldots \times [1 : 2^{nR_K}]$ and encoder 2, the backscatter device, assigns a codeword $b^n(m_0)$ to each message $m_0 \in [1 : 2^{nR_0}]$,

- K decoders, where decoder $i \in \{1, \ldots, K\}$ (or receiver, or user i) assigns an estimate $(\hat{m}_{0\to i}, \hat{m}_{K\to i} \ldots \hat{m}_{i+1\to i}, \hat{m}_{i\to i}) \in [1 : 2^{nR_0}] \times [1 : 2^{nR_K}] \times \ldots \times [1 : 2^{nR_{i+1}}] \times [1 : 2^{nR_i}]$, or an error message e to each received sequence y_i^n, where $\hat{m}_{j\to i}, j \in \{K, \ldots, i\}$ represents the estimation of m_j when decoded by receiver i.

We assume that the message, which is a $K+1$ tuple: $(M_0, M_1, \ldots, M_K)$, is uniformly distributed over $[1 : 2^{nR_0}] \times [1 : 2^{nR_1}] \times, \ldots, \times [1 : 2^{nR_K}]$. The average probability of error is then defined as $P_e^n = \mathbb{P}\Big\{ \bigcup_{\forall i} (\hat{M}_{0\to i}, \hat{M}_{i\to i}) \neq (M_0, M_i) \Big\}$.

Codebook generation.

Encoder 1: Fix the pmfs $p(u_K)p(u_{K-1}|u_K) \ldots p(x|u_2, \ldots, u_K)$.

i) First, randomly and independently generate 2^{nR_K} sequences $u_K^n(m_K) \in [1 : 2^{nR_K}]$ each according to $\prod_{i=1}^n p_{U_K(u_{i,K})}$.

ii) For each $m_{k+1} \in [1 : 2^{nR_{k+1}}], k \in \{K-1, K-2, \ldots, 2\}$ successively in this order, randomly and conditionally independently generate 2^{nR_k} sequences $u_k^n(m_k, m_{k+1}, \ldots, m_K)$, for all $m_k \in [1 : 2^{nR_k}]$, each according to $\prod_{i=1}^n p_{U_k|U_{k+1},\ldots,U_K}(u_{i,k}|u_{i,k+1}(m_{k+1}, \ldots, m_K), \ldots, u_{i,K}(m_K))$.

iii) For each $m_2 \in [1 : 2^{nR_2}]$ randomly and conditionally independently generate 2^{nR_1} sequences $x^n(m_1, \ldots, m_K), m_1 \in [1 : 2^{nR_1}]$ each according to $\prod_{i=1}^n p_{X|U_2,\ldots,U_K}(x_i|u_{i,2}(m_2, \ldots, m_K), \ldots, u_{i,K}(m_K))$. To send message $(m_1, \ldots, m_K)$, encoder 1 transmits codeword $x^n(m_1, \ldots, m_K)$.

Encoder 2: Randomly and independently generate 2^{nR_0} sequences $b^n(m_0), m_0 \in [1 : 2^{nR_0}]$, each according to $\prod_{i=1}^n p_B(b_i)$. To send message m_0, encoder 2 transmits codeword $b^n(m_0)$.

Decoding procedure.

Decoder K decides that $(\hat{m}_{0\to K}, \hat{m}_{K\to K})$ was sent, if it is the unique message pair such that $\{(u_K^n(\hat{m}_{K\to K}), b^n(\hat{m}_{0\to K}), y_K^n) \in \mathcal{T}_\epsilon^n\}$, where $\mathcal{T}_\epsilon^n$ is the set of ϵ-typical n-sequences; otherwise it declares an error.

Each decoder $i \in \{1, \ldots, K-1\}$ successively decodes the messages $m_j, j \in \{K, \ldots, i+1\}$ in this specific order by the following steps.

i) Each decoder i first jointly decodes U_K and B and decides that $(\hat{m}_{0\to i}, \hat{m}_{K\to i})$ was sent, if it is the unique pair such that $\{(u_K^n(\hat{m}_{K\to i}), b^n(\hat{m}_{0\to i}), y_i^n) \in \mathcal{T}_\epsilon^n\}$; otherwise it declares an error.

ii) If such $(\hat{m}_{0\to i}, \hat{m}_{K\to i})$ is found, decoder i declares that $\hat{m}_{i\to i}$ is sent if it is the unique message such that $\{(u_K^n(\hat{m}_{K\to i}), u_{K-1}^n(\hat{m}_{K-1\to i}, \hat{m}_{K\to i}), \ldots, u_i^n(\hat{m}_{i\to i}, \ldots, \hat{m}_{K\to i}), b^n(\hat{m}_{0\to i}), y_i^n) \in \mathcal{T}_\epsilon^n\}$, where the estimates $\hat{m}_{j\to i}, j \in \{K-1, \ldots, i+1\}$ are obtained in a successive manner starting from $\hat{m}_{K-1\to i}$ to $\hat{m}_{i+1\to i}$ as decoder i declares that $\hat{m}_{j\to i}, j \in \{K-1, \ldots, i+1\}$ is sent if it is the unique message such that $\{(u_K^n(\hat{m}_{K\to i}), u_{K-1}^n(\hat{m}_{K-1\to i}, \hat{m}_{K\to i}), \ldots, u_j^n(\hat{m}_{j\to i}, \ldots, \hat{m}_{K\to i}), b^n(\hat{m}_{0\to i}), y_i^n) \in \mathcal{T}_\epsilon^n\}$; otherwise it declares an error. Note that whenever an error has been declared, the decoding process stops.

Analysis of the probability of error.

Assume without loss of generality that the message $(M_0 = M_1 = \ldots = M_K = 1)$ was sent [30]. By the symmetry of code generation, the probability of error averaged over all possible codebooks and messages is: $\mathbb{P}(\varepsilon) = \mathbb{P}(\varepsilon | M_0 = M_1 = \ldots = M_K = 1)$.

Let us focus on the decoder $i \in \{1, \ldots, K\}$. In the SIC decoding procedure, decoder i first decodes messages destined

to receivers $j \in \{K, K-1, \ldots, i+1\}$ before decoding its own message. Hence, decoder i declares an error if at least one of the following error events occurs:

$$\begin{aligned}
\varepsilon_{i,1} &= \{(u_K^n(1), b^n(1), y_i^n) \notin \mathcal{T}_\epsilon^n\}, \textit{non-joint typicality;}\\
\varepsilon_{i,2} &= \{(u_K^n(1), b^n(m_{0\to i}), y_i^n) \in \mathcal{T}_\epsilon^n,\ m_{0\to i} \neq 1\},\\
&\quad m_{0\to i} \textit{ not successfully decoded;}\\
\varepsilon_{i,3} &= \{(u_K^n(m_{K\to i}), b^n(1), y_i^n) \in \mathcal{T}_\epsilon^n,\ m_K \neq 1\},\\
&\quad m_{K\to i} \textit{ not successfully decoded;}\\
\varepsilon_{i,4} &= \{(u_K^n(m_{K\to i}), b^n(m_{0\to i}), y_i^n) \in \mathcal{T}_\epsilon^n, m_{0\to i} \neq 1,\\
&\quad m_{K\to i} \neq 1\}, \quad m_{0\to i} \textit{ and } m_{K\to i} \textit{ not successfully decoded;}\\
\varepsilon_{i,j,5} &= \{(u_K^n(1), \ldots, u_j^n(1, \ldots, 1), b^n(1), y_i^n) \notin \mathcal{T}_\epsilon^n,\\
&\quad i+1 \leq j \leq K-1\}, \quad \textit{non-joint typicality;}\\
\varepsilon_{i,j,6} &= \{(u_K^n(1), \ldots, u_j^n(m_{j\to i}, 1, \ldots, 1), b^n(1), y_i^n) \in \mathcal{T}_\epsilon^n,\\
&\quad m_{j\to i} \neq 1\}, \quad m_{j\to i} \textit{ not successfully decoded;}\\
\varepsilon_{i,i,7} &= \{(u_K^n(1), \ldots, u_i^n(m_{i\to i}, 1, \ldots, 1), b^n(1), y_i^n) \notin \mathcal{T}_\epsilon^n\},\\
&\quad \textit{non-joint typicality;}\\
\varepsilon_{i,i,8} &= \{(u_K^n(1), \ldots, u_i^n(m_{i\to i}, 1, \ldots, 1), b^n(1), y_i^n) \in \mathcal{T}_\epsilon^n,\\
&\quad m_{i\to i} \neq 1\}, \quad m_{i\to i} \textit{ not successfully decoded.}
\end{aligned}$$

By the union bound of events, we obtain $\mathbb{P}(\varepsilon_i) \leq \mathbb{P}(\varepsilon_{i,1}) + \ldots + \mathbb{P}(\varepsilon_{i,i,8})$. Let us now bound each term individually. By the law of large numbers (LLN), the probabilities $\mathbb{P}(\varepsilon_{i,1})$, $\mathbb{P}(\varepsilon_{i,j,5})$ and $\mathbb{P}(\varepsilon_{i,i,7})$ can be shown to tend to zero as $n \to \infty$. By the packing lemma [30, Lemma 3.1], $\mathbb{P}(\varepsilon_{i,2})$ tends to zero as $n \to \infty$ if $R_{0\to i} \leq \mathbb{I}(B; U_K, Y_i) - \delta(\epsilon)$, where $\delta(\epsilon)$ is a function that goes to zero when $\epsilon \to 0$. Furthermore, since B is independent of U_K, then $\mathbb{I}(B; U_K, Y_i) = \mathbb{I}(B; Y_i|U_K)$. Hence, $\mathbb{P}(\varepsilon_{i,2})$ tends to zero as $n \to \infty$ if $R_{0\to i} \leq \mathbb{I}(B; Y_i|U_K) - \delta(\epsilon),\ \forall\ 1 \leq i \leq K$. Similarly, the error probabilities $\mathbb{P}(\varepsilon_{i,3})$, $\mathbb{P}(\varepsilon_{i,4})$, $\mathbb{P}(\varepsilon_{i,j,6})$, and $\mathbb{P}(\varepsilon_{i,i,8})$ tend to zero as $n \to \infty$, if the following conditions are met

$$R_{K\to i} \leq \mathbb{I}(U_K; Y_i|B) - \delta(\epsilon),\ \forall\ 1 \leq i \leq K, \quad (19)$$

$$R_{0\to i} + R_{K\to i} \leq \mathbb{I}(U_K, B; Y_i) - \delta(\epsilon),\ \forall\ 1 \leq i \leq K, \quad (20)$$

$$R_{j\to i} \leq \mathbb{I}(U_j; Y_i|B, U_K, \ldots, U_{j+1}) - \delta(\epsilon),\ \forall\ 1 \leq j \leq K-1, \forall i < j, \quad (21)$$

$$R_{i\to i} \leq \mathbb{I}(U_i; Y_i|B, U_K, \ldots, U_{i+1}) - \delta(\epsilon),\ \forall\ 1 \leq i \leq K-1. \quad (22)$$

The message intended for receiver $j \in \{1, \ldots, K-1\}$ is decoded by receivers $i \in \{1, \ldots, j-1\}$ and receiver j with a data rate $R_{j\to i}$ and $R_{j\to j}$, respectively. Therefore the achievable data rate for decoding M_j is $R_j \leq \min_{i<j}(R_{j\to i}, R_{j\to j}) \overset{(a)}{=} \min_{i\leq j} \mathbb{I}(U_j; Y_i|B, U_K, \ldots, U_{i+1}), \forall\ 1 \leq j \leq K-1$, where (a) follows from (21) and (22). Further, the achievable rate for decoding M_0 and M_K are defined as $R_0 \leq \min\limits_{1\leq i\leq K} R_{0\to i}$ and $R_K \leq \min\limits_{1\leq i\leq K} R_{K\to i}$ and are constrained as

$$R_0 \leq \min_{1\leq i\leq K} \mathbb{I}(B; Y_i|U_K), \quad R_K \leq \min_{1\leq i\leq K} \mathbb{I}(U_K; Y_i|B),$$
$$R_0 + R_K \leq \min_{1\leq i\leq K} \mathbb{I}(U_K, B; Y_i),$$

which completes the proof of Theorem 1.

B. Proof of Theorem 2 (Gaussian channels)

From Lemma (1), the achievable rate for decoding the message destined to receiver j satisfies

$$R_j \leq \min_{i\leq j}\ \mathbb{I}(U_j; Y_i|B, U_K, \ldots, U_{j+1}),\ \forall 1 \leq j \leq K-1, \quad (23)$$

$$\overset{(b)}{=} qC\left(\min_{i\leq j}(\gamma_{j\to i|1})\right) + (1-q)C\left(\min_{i\leq j}(\gamma_{j\to i|0})\right), \quad (24)$$
$$\forall\ 1 \leq j \leq K-1,$$

where (b) follows from $B \sim \text{Bern(q)}$, $U_k \sim \mathcal{N}(0, p_k)$, $\forall k \in \{2, ..., K\}$ and $X = \sum_{k=2}^K U_k + V$, with $V \sim \mathcal{N}(0, p_1)$, which maximizes the mutual information expressions in (23) and yields the capacity of the point-to-point AWGN channel when decoding the message intended to receiver j at decoder i in the reflecting state ($B = 1$) and transparent state ($B = 0$) respectively.

Following similar steps as above, we obtain the achievable rates R_K and R_0 as

$$\begin{aligned}
R_K &\leq qC\left(\min_i(\gamma_{K\to i|1})\right) + (1-q)C\left(\min_i(\gamma_{K\to i|0})\right),\\
R_0 &\leq \min_{1\leq i\leq K} \mathbb{H}(Y_i|U_K) - \frac{q}{2}\log_2\left(2\pi e\sigma_i^2\left(H_{i|1}(\rho)\sum_{k=1}^{K-1} p_k + 1\right)\right)\\
&\quad - \frac{1-q}{2}\log_2\left(2\pi e\sigma_i^2\left(H_{i|0}\sum_{k=1}^{K-1} p_k + 1\right)\right),
\end{aligned}$$

which concludes the proof of Theorem 2.

Appendix B
Proof of Theorem 3 (optimal power allocation)

A. Convexity of (EE2)

We start by showing that ($\mathbf{EE2}$) is a convex optimization problem. For this, we analyze its objective function $\eta_{EE}(\mathbf{p})$ whose second-order partial derivative w.r.t. $p_i,\ p_j,\ \forall i, j$, equals

$$\frac{\partial^2 \eta_{EE}(\mathbf{p})}{\partial p_j \partial p_i} = \begin{cases} d_j, & \text{if } j \geq i \\ d_i, & \text{otherwise,} \end{cases}$$

where

$$\begin{aligned}
d_j &= \sum_{k=j}^{K-1} \frac{q}{2\ln 2}\left(\frac{(H_{k+1|1})^2}{\left(1+H_{k+1|1}\theta_k(\mathbf{p})\right)^2} - \frac{(H_{k|1})^2}{\left(1+H_{k|1}\theta_k(\mathbf{p})\right)^2}\right)\\
&\quad + \sum_{k=j}^{K-1} \frac{(1-q)}{2\ln 2}\left(\frac{(H_{k+1|0})^2}{\left(1+H_{k+1|0}\theta_k(\mathbf{p})\right)^2} - \frac{(H_{k|0})^2}{\left(1+H_{k|0}\theta_k(\mathbf{p})\right)^2}\right)\\
&\quad - \frac{q}{2\ln 2} \times \frac{(H_{K|1})^2}{\left(1+H_{K|1}\theta_K(\mathbf{p})\right)^2} - \frac{(1-q)}{2\ln 2} \times \frac{(H_{K|0})^2}{\left(1+H_{K|0}\theta_K(\mathbf{p})\right)^2}.
\end{aligned}$$

Let $\mathbf{D}$ be the Hessian matrix and let us show that $\mathbf{T} = -\mathbf{D}$ is positive semi-definite by proving that all of its leading principal minors are positive, i.e., $\det\ \mathbf{T}[1:j, 1:j] \geq 0, \forall j \in \{1, ..., K\}$.

Note that since $H_{k|1} \geq H_{k+1|1}$ and $H_{k|0} \geq H_{k+1|0}, \forall k \in \{1, \ldots, K-1\}$, we can show that $d_j \leq 0$, for all j and that $d_{k+1} - d_k \geq 0, \forall k$. The first leading principal minor is $\det\ \mathbf{T}[1,1] = -d_1 \geq 0$. For $1 < j \leq K$, the j-th leading principal minor equals $\det\ \mathbf{T}[1:j, 1:j] = -d_j \prod_{k=1}^{j-1}(d_{k+1} - d_k) \geq 0$. Therefore, all leading principal

minors of $\mathbf{T}$ are positive, which implies that $\mathbf{T} \succeq 0$ equivalent to the Hessian matrix $\mathbf{D} \preceq 0$. The latter means that the objective function is jointly concave w.r.t. $\mathbf{p} = (p_1, \ldots, p_K)$. Now, given the above and that all the inequality constraints are affine w.r.t. $\mathbf{p}$, the optimization problem $(\mathbf{EE2})$ is convex.

*B. Solving the KKT conditions for **(EE2)** when $H_{1|0} > H_{2|0}$ or $H_{1|1} > H_{2|1}$*

The associated Lagrangian function of the optimization problem $(\mathbf{EE2})$ is given by

$$\mathcal{L}(\rho^*, \mathbf{p}) = \sum_{k=1}^{K} R_k(\rho^*, \mathbf{p}) - \alpha(\theta_K(\mathbf{p}) + P_{\mathrm{c}}) + \lambda(P_{\max} - \theta_K(\mathbf{p})) + \sum_{k=1}^{K} \beta_k \left(\theta_k(\mathbf{p}) - A_k \theta_{k-1}(\mathbf{p}) + \frac{(A_k - 1)}{H_{k|0}} \right),$$

where λ and $\boldsymbol{\beta} = [\beta_1, ..., \beta_K]$ are the non-negative Lagrange multipliers associated with the constraints $(C1)$ and $(C2a)$ respectively. The necessary and sufficient KKT optimality conditions are

$$\begin{cases} \frac{\partial \mathcal{L}}{\partial p_i} \triangleq \sum_{k=i}^{K-1} \frac{q}{2\ln 2} \left(\frac{H_{k|1}}{1+H_{k|1}\theta_k(\mathbf{p})} - \frac{H_{k+1|1}}{1+H_{k+1|1}\theta_k(\mathbf{p})} \right) \\ \quad + \sum_{k=i}^{K-1} \frac{(1-q)}{2\ln 2} \left(\frac{H_{k|0}}{1+H_{k|0}\theta_k(\mathbf{p})} - \frac{H_{k+1|1}}{1+H_{k+1|1}\theta_k(\mathbf{p})} \right) \\ \quad + \frac{q}{2\ln 2} \times \frac{H_{K|1}}{1+H_{K|1}\theta_K(\mathbf{p})} + \frac{(1-q)}{2\ln 2} \times \frac{H_{K|0}}{1+H_{K|0}\theta_K(\mathbf{p})} \\ \quad -(\alpha+\lambda) + \sum_{k=i}^{K} \beta_k - \sum_{k=i}^{K-1} (A_{k+1}\beta_{k+1}) = 0, & (K1) \\ \lambda(P_{max} - \theta_K(\mathbf{p})) = 0, & (K2) \\ \beta_k \left(\theta_k(\mathbf{p}) - A_k \theta_{k-1}(\mathbf{p}) + \frac{(A_k-1)}{H_{k|0}} \right) = 0, & (K3) \\ (C1'), (C2'), \lambda \geq, \boldsymbol{\beta} \geq 0, & (K4) \end{cases}$$

From $(K1)$, and by using the difference between two consecutive derivatives, $(\frac{\partial \mathcal{L}}{\partial p_i} - \frac{\partial \mathcal{L}}{\partial p_{i+1}}) = 0$

$$\frac{q}{2\ln 2} \left(\frac{H_{i|1}}{1+H_{i|1}\theta_i(\mathbf{p})} - \frac{H_{i+1|1}}{1+H_{i+1|1}\theta_i(\mathbf{p})} \right) + \frac{(1-q)}{2\ln 2} \left(\frac{H_{i|0}}{1+H_{i|0}\theta_i(\mathbf{p})} - \frac{H_{i+1|0}}{1+H_{i+1|0}\theta_i(\mathbf{p})} \right) + \beta_i = A_{i+1}\beta_{i+1}. \quad (25)$$

We know that $H_{i|1} \geq H_{i+1|1},\ H_{i|0} \geq H_{i+1|0},\ A_{i+1} > 0$ and $\beta_{i+1} \geq 0, \quad \forall i \in \{1, \ldots, K-1\}$. We discuss the two cases below:

i) If $H_{1|0} > H_{2|0}$, by replacing $i = 1$ in (25), since $A_2 > 0$, we have $\beta_2 > 0$. For $i = 2$, since $\beta_2 > 0$ and $A_3 > 0$ we obtain $\beta_3 > 0$. Recursively, for all $i \geq 2$ we find $\beta_i > 0$. Using $(K3)$, we obtain $\theta_k(\mathbf{p}) = A_k\theta_{k-1}(\mathbf{p}) - \frac{(A_k-1)}{H_{k|0}}, \forall k \geq 2$. This means that all receivers $k \geq 2$ will be allocated a power to meet exactly their QoS requirement. By induction, we find that

$$\theta_k(\mathbf{p}) = \theta_1(\mathbf{p}) \prod_{i=2}^{k} A_i + \sum_{i=2}^{k-1} \frac{(A_i-1)}{H_{i|0}} \prod_{j=i+1}^{k} A_j + \frac{(A_k-1)}{H_{k|0}}, \forall k \geq 2. \quad (26)$$

Notice that all variables θ_k are expressed in terms of $\theta_1(\mathbf{p}) = p_1$. Hence, we obtain the expressions of the optimal powers $p_k^*, \forall k \geq 2$ in closed form as functions of p_1 as in Theorem 3.

ii) In the case where $H_{1|0} = H_{2|0}$, the first order partial derivatives of $\eta_{EE}(\mathbf{p})$ write as

$$\frac{\partial \eta_{EE}}{\partial p_i} = \begin{cases} \Upsilon(\mathbf{p}) \triangleq \sum_{k=i}^{K-1} \frac{q}{2\ln 2} \left(\frac{H_{k|1}}{1+H_{k|1}\theta_k(\mathbf{p})} - \frac{H_{k+1|1}}{1+H_{k+1|1}\theta_k(\mathbf{p})} \right) \\ + \sum_{k=i}^{K-1} \frac{(1-q)}{2\ln 2} \left(\frac{H_{k|0}}{1+H_{k|0}\theta_k(\mathbf{p})} - \frac{H_{k+1|0}}{1+H_{k+1|0}\theta_k(\mathbf{p})} \right) \\ + \frac{q}{2\ln 2} \times \frac{H_{K|1}}{1+H_{K|1}\theta_K(\mathbf{p})} + \frac{(1-q)}{2\ln 2} \times \frac{H_{K|0}}{1+H_{K|0}\theta_K(\mathbf{p})}, & \text{if } i \geq 2 \\ \Upsilon(\mathbf{p}) + \frac{q}{2\ln 2} \left(\frac{H_{1|1}}{1+H_{1|1}\theta_1(\mathbf{p})} - \frac{H_{2|1}}{1+H_{2|1}\theta_1(\mathbf{p})} \right), & \text{if } i = 1. \end{cases}$$

In this case, the difference between two consecutive derivatives of the Lagrange function gives

$$\frac{q}{2\ln 2} \left(\frac{H_{1|1}}{1+H_{1|1}\theta_1(\mathbf{p})} - \frac{H_{2|1}}{1+H_{2|1}\theta_1(\mathbf{p})} \right) + \beta_1 = A_2\beta_2,$$
$$\frac{q}{2\ln 2} \left(\frac{H_{i|1}}{1+H_{i|1}\theta_i(\mathbf{p})} - \frac{H_{i+1|1}}{1+H_{i+1|1}\theta_i(\mathbf{p})} \right) + \frac{(1-q)}{2\ln 2} \left(\frac{H_{i|0}}{1+H_{i|0}\theta_i(\mathbf{p})} - \frac{H_{i+1|0}}{1+H_{i+1|0}\theta_i(\mathbf{p})} \right) + \beta_i = A_{i+1}\beta_{i+1}.$$

We discuss two cases:

i) If $H_{1|1} > H_{2|1}$ then, since $\beta_1 \geq 0$ and $A_2 > 0$, we have $\beta_2 > 0$ and recursively we find $\beta_i > 0, \forall i \geq 2$, which leads to the analytical closed-form expressions of $p_k^*, \forall k \geq 2$ as functions of p_1 and given in Theorem 3, as in the case $H_{1|0} > H_{2|0}$.

ii) If $H_{1|1} = H_{2|1}$, the analysis of the solution $\mathbf{p}^*$ is delegated to the end of the appendix.

C. Finding the optimal power allocated to user 1 when $H_{1|0} > H_{2|0}$ or $H_{1|1} > H_{2|1}$

Using the above optimal expressions $p_k^*, \forall k \geq 2$ as functions of p_1, we can reformulate the multi-variable optimization problem $(\mathbf{EE2})$ into a simple single-variable optimization problem

$$(\mathbf{EE3}) \quad \max_{\ell \leq p_1 \leq u} f_1(p_1) \triangleq \sum_{k=1}^{K} \frac{q}{2} \log_2 \left(\frac{1+H_{k|1}\theta_k(\mathbf{p})}{1+H_{k|1}\theta_{k-1}(\mathbf{p})} \right) + \frac{(1-q)}{2} \log_2 \left(1+H_{1|0}p_1\right) + \sum_{k=2}^{K} (1-q) R_k^{\min} - \alpha \left(p_1 \prod_{i=2}^{K} A_i + \sum_{i=2}^{K-1} \frac{(A_i-1)}{H_{i|0}} \prod_{j=i+1}^{K} A_j + \frac{(A_K-1)}{H_{K|0}} + P_{\mathrm{c}} \right) \quad (27)$$

where $\ell = \frac{(A_1-1)}{H_{1|0}}$ and $u = \left(P_{\max} - P_{\min} + \ell \prod_{j=2}^{K} A_j \right) \Big/ \prod_{i=2}^{K} A_i$. The optimal solution of $(\mathbf{EE3})$ is given by $p_1^*(\alpha) = \max\left(\min\left(\overline{p_1}(\alpha); u\right); \ell\right)$ where $\overline{p_1}(\alpha)$ is the critical point of the objective satisfying $\frac{\partial f_1(p_1)}{\partial p_1} = 0$ and can be found numerically.

D. The case in which $H_{1|0} = H_{2|0}$ and $H_{1|1} = H_{2|1}$

The expression of $\eta_{EE}(\mathbf{p})$ simplifies in this case. The main trick is to consider receiver 1 and 2 as a single entity, having the strongest channel gains $H'_{1|0} = H_{1|0} = H_{2|0}$ and $H'_{1|1} = H_{1|1} = H_{2|1}$, and whose achievable data rate and allocated power are considered as $R'_1 = (R_1 + R_2)$ and $p'_1 = p_1 + p_2$ respectively. Having done this variable change, the same discussion follows subsequently as in the previous subsections of Appendix B; two cases arise: i) $H'_{1|0} = H_{3|0}$ and $H'_{1|1} = H_{3|1}$, and ii) $H'_{1|0} > H_{3|0}$ or $H'_{1|1} > H_{3|1}$. In the latter, we obtain the analytical closed-form expressions of $p_k^*, \forall k \geq 3$ as a function of p'_1 and $(p'_1)^*$ is obtained by solving the resulting $(\mathbf{EE3})$ problem. Then, we can split the power $(p'_1)^*$ such that p_2^* is the enough power required to satisfy the QoS requirement for receiver 2, and the remaining power $p_1^* = (p'_1)^* - p_2^*$. In the former case, a recurring reasoning can be applied etc. Finally, the same reasoning applies in the extreme symmetric case in which $H_{1|0} = H_{2|0} = \ldots = H_{K|0}$ and $H_{1|1} = H_{2|1} = \ldots =$

$H_{K|1}$. Note that such a symmetric case is quite unlikely to occur in practice. Moreover, NOMA in this case would likely not outperform OMA.

For simplicity and given that the main ideas behind the proof are explained in the previous subsections of Appendix B, we have included only the asymmetric channel cases in Theorem 3.

REFERENCES

[1] H. El Hassani, A. Savard, E. V. Belmega, and R. C. De Lamare, "Energy-efficient cooperative backscattering closed-form solution for NOMA," in *IEEE GLOBECOM*, 2021, pp. 1–6.

[2] D. C. Nguyen, M. Ding, P. N. Pathirana, A. Seneviratne, J. Li, D. Niyato, O. Dobre, and H. V. Poor, "6G internet of things: A comprehensive survey," *IEEE Internet Things J.*, 2021.

[3] M. Vaezi, Z. Ding, and H. V. Poor, *Multiple access techniques for 5G wireless networks and beyond*. Springer, 2019.

[4] Y. Saito, Y. Kishiyama, A. Benjebbour, T. Nakamura, A. Li, and K. Higuchi, "Non-orthogonal multiple access (NOMA) for cellular future radio access," in *IEEE VTC Spring*, 2013, pp. 1–5.

[5] H. El Hassani, A. Savard, and E. V. Belmega, "A closed-form solution for energy-efficiency optimization in multi-user downlink NOMA," in *IEEE PIMRC*, 2020, pp. 1–5.

[6] F. M. Al-Turjman, M. Imran, and S. T. Bakhsh, "Energy efficiency perspectives of femtocells in internet of things: Recent advances and challenges," *IEEE Access*, vol. 5, pp. 26 808–26 818, 2017.

[7] V. Liu, A. Parks, V. Talla, S. Gollakota, D. Wetherall, and J. R. Smith, "Ambient backscatter: Wireless communication out of thin air," *ACM SIGCOMM Computer Communication Review*, vol. 43, no. 4, pp. 39–50, 2013.

[8] N. Van Huynh, D. T. Hoang, X. Lu, D. Niyato, P. Wang, and D. I. Kim, "Ambient backscatter communications: A contemporary survey," *IEEE Commun. Surveys Tuts.*, vol. 20, no. 4, pp. 2889–2922, 2018.

[9] Y. Kokar, D.-T. Phan-Huy, R. Fara, K. Rachedi, A. Ourir, J. de Rosny, M. Di Renzo, J.-C. Prévotet, and M. Helard, "First experimental ambient backscatter communication using a compact reconfigurable tag antenna," in *IEEE Globecom Workshops*, 2019, pp. 1–6.

[10] C. Song, Y. Ding, A. Eid, J. G. Hester, X. He, R. Bahr, A. Georgiadis, G. Goussetis, and M. M. Tentzeris, "Advances in wirelessly powered backscatter communications: From antenna/RF circuitry design to printed flexible electronics," *Proceedings of the IEEE*, vol. 110, no. 1, pp. 171–192, 2021.

[11] G. Wang, F. Gao, R. Fan, and C. Tellambura, "Ambient backscatter communication systems: Detection and performance analysis," *IEEE Trans. Commun.*, vol. 64, no. 11, pp. 4836–4846, 2016.

[12] J. Qian, F. Gao, G. Wang, S. Jin, and H. Zhu, "Noncoherent detections for ambient backscatter system," *IEEE Trans. Wireless Commun.*, vol. 16, no. 3, pp. 1412–1422, 2016.

[13] S. Zhou, W. Xu, K. Wang, C. Pan, M.-S. Alouini, and A. Nallanathan, "Ergodic rate analysis of cooperative ambient backscatter communication," *IEEE Wireless Commun. Lett.*, vol. 8, no. 6, pp. 1679–1682, 2019.

[14] W. Liu, Y.-C. Liang, Y. Li, and B. Vucetic, "Backscatter multiplicative multiple-access systems: Fundamental limits and practical design," *IEEE Trans. Wireless Commun.*, vol. 17, no. 9, pp. 5713–5728, 2018.

[15] J. K. Devineni and H. S. Dhillon, "Ambient backscatter systems: Exact average bit error rate under fading channels," *IEEE Trans. Green Commun. Netw.*, vol. 3, no. 1, pp. 11–25, 2018.

[16] X. Jia and X. Zhou, "Performance characterization of relaying using backscatter devices," *IEEE Open J. Commun. Soc.*, vol. 1, pp. 819–834, 2020.

[17] X. Kang, Y.-C. Liang, and J. Yang, "Riding on the primary: A new spectrum sharing paradigm for wireless-powered IoT devices," *IEEE Trans. Wireless Commun.*, vol. 17, no. 9, pp. 6335–6347, 2018.

[18] Y. Ye, L. Shi, R. Qingyang Hu, and G. Lu, "Energy-efficient resource allocation for wirelessly powered backscatter communications," *IEEE Commun. Lett.*, vol. 23, no. 8, pp. 1418–1422, 2019.

[19] B. Lyu, C. You, Z. Yang, and G. Gui, "The optimal control policy for RF-powered backscatter communication networks," *IEEE Trans. Veh. Technol.*, vol. 67, no. 3, pp. 2804–2808, 2017.

[20] W. Chen, H. Ding, S. Wang, D. B. da Costa, F. Gong, and P. H. J. Nardelli, "Backscatter cooperation in NOMA communications systems," *IEEE Trans. Wireless Commun.*, vol. 20, no. 6, pp. 3458–3474, 2021.

[21] Y. Xu, Z. Qin, G. Gui, H. Gacanin, H. Sari, and F. Adachi, "Energy efficiency maximization in NOMA enabled backscatter communications with QoS guarantee," *IEEE Wireless Commun. Lett.*, vol. 10, no. 2, pp. 353–357, 2020.

[22] W. U. Khan, X. Li, M. Zeng, and O. A. Dobre, "Backscatter-enabled NOMA for future 6G systems: A new optimization framework under imperfect SIC," *IEEE Commun. Lett.*, vol. 25, no. 5, pp. 1669–1672, 2021.

[23] W. U. Khan, M. A. Javed, T. N. Nguyen, S. Khan, and B. M. Elhalawany, "Energy-efficient resource allocation for 6G backscatter-enabled NOMA IoV networks," *IEEE Trans. Intell. Transp. Syst.*, 2021.

[24] S. Gong, X. Huang, J. Xu, W. Liu, P. Wang, and D. Niyato, "Backscatter relay communications powered by wireless energy beamforming," *IEEE Trans. Commun.*, vol. 66, no. 7, pp. 3187–3200, 2018.

[25] R. Fara, D.-T. Phan-Huy, and M. Di Renzo, "Ambient backscatters-friendly 5G networks: creating hot spots for tags and good spots for readers," in *IEEE WCNC*, 2020, pp. 1–7.

[26] W. Zhao, G. Wang, S. Atapattu, C. Tellambura, and H. Guan, "Outage analysis of ambient backscatter communication systems," *IEEE Commun. Lett.*, vol. 22, no. 8, pp. 1736–1739, 2018.

[27] A. W. Nazar, S. A. Hassan, H. Jung, A. Mahmood, and M. Gidlund, "BER analysis of a backscatter communication system with non-orthogonal multiple access," *IEEE Trans. Green Commun. Netw.*, vol. 5, no. 2, pp. 574–586, 2021.

[28] P. Li, R. C. De Lamare, and R. Fa, "Multiple feedback successive interference cancellation detection for multiuser MIMO systems," *IEEE Trans. Wireless Commun.*, vol. 10, no. 8, pp. 2434–2439, 2011.

[29] T. M. Cover, "Thomas. elements of information theory," *Wiley Series in Telecommunications*, 1991.

[30] A. El Gamal and Y.-H. Kim, *Network information theory*. Cambridge university press, 2011.

[31] A. Zappone and E. Jorswieck, "Energy efficiency in wireless networks via fractional programming theory," *Foundations and Trends in Communications and Information Theory*, vol. 11, no. 3-4, pp. 185–396, 2015.

[32] R. Masmoudi, E. V. Belmega, I. Fijalkow, and N. Sellami, "A unifying view on energy-efficiency metrics in cognitive radio channels," in *IEEE EUSIPCO*, 2014, pp. 171–175.

[33] Z. Ding, R. Schober, and H. V. Poor, "Unveiling the importance of SIC in NOMA systems—Part II: New results and future directions," *IEEE Commun. Lett.*, vol. 24, no. 11, pp. 2378–2382, 2020.

[34] S. P. Boyd and L. Vandenberghe, *Convex optimization*. Cambridge University Press, 2004.

Hajar El Hassani (IEEE S'21) is currently a post-doctoral researcher at L2S laboratory, CNRS, CentraleSupélec in France, working on modeling and optimization of wireless communications with an application to Reconfigurable Intelligent Surfaces. She received her PhD degree from CY Cergy Paris University in 2022. In 2019, she received the Engineer's Diploma of Telecommunication and Network Engineering from ENSA in Khouribga, Morocco. In 2018, she received the Huawei scholarship program: Seeds for the Future. Her research interests include green and energy-efficient communications, resource allocation, convex optimization and machine learning applied to wireless communications.

Anne Savard (IEEE S'14, M'17) received the engineer degree from ENSEA, Cergy-Pontoise, France in 2012, and the M.Sc. and Ph.D. degrees both from the University of Cergy-Pontoise in 2012 and 2015 respectively. From October 2015 to August 2016, she held a post-doctoral fellowship at Georgia Institute of Technology, USA. Since September 2016, she is an Associate Professor at IMT Nord Europe, France. Her research interests lie in multi-user information theory, cooperative communications, resource allocation problems and channel coding. From 2020 to 2023, she served on the editorial board of the Transactions on Emerging Telecommunications Technologies (ETT). Since 2023, she serves on the editorial board of the IEEE Transactions on Machine Learning in Communications and Networking.

E. Veronica Belmega (IEEE S'08, M'10, SM'20) is a full professor at the Université Gustave Eiffel and LIGM laboratory, Marne-la-Vallée, France, since May 2022. Previously, she was an associate professor (MCF HDR) with ENSEA graduate school (Sep. 2011 - Apr. 2022) and Deputy Director of ETIS laboratory (Jan. 2020 - Apr. 2022), Cergy, France. She received the M.Sc. (engineering) degree from the University Politehnica of Bucharest, Romania, in 2007, and the M.Sc. and Ph.D. degrees both from the University Paris-Sud 11, Orsay, France, in 2007 and 2010. From 2010 to 2011, she was a Post-doctoral researcher in a joint project between Princeton University, N.J., USA and Supélec, France. In 2015-2017, she was a visiting researcher at Inria, France. In 2009, she received the L'Oréal – UNESCO – French Academy of Science national fellowship and, in 2021, she received the CY Alliance award For Women in Science, France. In between 2018-2022, she received the Doctoral Supervision and Research Bonus (PEDR) by the French National Council of Universities (CNU 61). She served as Executive Editor of Trans. on Emerging Telecommun. Technologies (ETT) in 2016-2020; among the Top Editors 2016-2017. She currently serves as Area Editor for the IEEE TRANSACTIONS ON MACHINE LEARNING IN COMMUNICATIONS AND NETWORKING. She is Principal Investigator and Scientific Coordinator of the ANR-FAPESP French-Brazilian project "ELIOT: Enabling Technologies for IoT". Her research interests lie in convex optimization, game theory and machine learning applied to distributed wireless communication and power networks; areas in which she has co-authored over 80 papers in international journals and conferences.
https://sites.google.com/site/evbelmega/home

Rodrigo C. de Lamare was born in Rio de Janeiro, Brazil, in 1975. He received his Diploma in electronic engineering from the Federal University of Rio de Janeiro in 1998 and the MSc and PhD degrees in electrical engineering from the Pontifical Catholic University of Rio de Janeiro (PUC-Rio) in 2001 and 2004, respectively. Since January 2006, he has been with the Communications Group, School of Physics, Engineering and Technology, University of York, United Kingdom, where he is a Professor. Since April 2013, he has also been a Professor at PUC-RIO. Dr de Lamare is a senior member of the IEEE and an elected member of the IEEE Signal Processing for Communications and Networking Committee. He served as editor for IEEE Wireless Communications Letters and IEEE Transactions on Communications. His research interests lie in communications and signal processing, areas in which he has published over 500 papers in international journals and conferences.